

Title: A new approach to predict progression-free survival in stage IV EGFR-mutant NSCLC patients with EGFR-TKI therapy

Authors' names and degrees

Jiangdian Song^{1,2,3#}, Jingyun Shi^{4#}, Di Dong^{1,5#}, Mengjie Fang^{1,5}, Wenzhao Zhong⁶, Kun Wang^{1,5}, Ning Wu⁷, Yanqi Huang⁸, Zhenyu Liu^{1,5}, Yue Cheng⁹, Yuncui Gan⁹, Yongzhao Zhou⁹, Ping Zhou⁹, Bojiang Chen⁹, Changhong Liang⁸, Zaiyi Liu^{8*}, Weimin Li^{9*}, Jie Tian^{1,5,10*}

these authors contributed equally to the work.

Authors' affiliations

1. CAS Key Laboratory of Molecular Imaging, Institute of Automation, Chinese Academy of Sciences, Beijing, China.
2. School of Medical Informatics, China Medical University, Shenyang, Liaoning, China.
3. Sino-Dutch Biomedical and Information Engineering School, Northeastern University, Shenyang, Liaoning, China.
4. Department of Radiology, Shanghai Pulmonary Hospital, Tongji University School of Medicine, Shanghai, China
5. University of Chinese Academy of Sciences, Beijing, China.
6. Guangdong Lung Cancer Institute, Guangdong General Hospital, Guangdong Academy of Medical Sciences, Guangzhou, China
7. PET-CT center, National Cancer Center/Cancer Hospital, Chinese Academy of Medical Sciences and Peking Union Medical College, Beijing, China.
8. Department of Radiology, Guangdong General Hospital, Guangdong Academy of Medical Sciences, Guangzhou, China.
9. Department of Respiratory and Critical Care Medicine, West China Hospital, Chengdu, China
10. Beijing Key Laboratory of Molecular Imaging, Beijing, China.

Running title

Prediction of EGFR-TKI treatment outcome in stage IV NSCLC

Financial support

This work was supported by grants from the Natural Science Foundation of China (81771924, 81501616, 61671449, 61231004, 81671854, 81501549), National Key R&D Program of China (2017YFA0205200, 2017YFC1308700, 2017YFC1308701, 2017YFC1309100), the Science and Technology Service Network Initiative of the Chinese Academy of Sciences (KFJ-SW-STS-160), the Instrument Developing Project of the Chinese Academy of Sciences (YZ201502), the Beijing Municipal Science and Technology Commission (Z171100000117023, Z161100002616022), and the Youth Innovation Promotion Association CAS.

Keywords

pre-therapy CT; NSCLC; progression-free survival; EGFR-TKI; risk stratification.

Declaration of Interests

The authors declare no potential conflicts of interest.

***Corresponding authors**

Zaiyi Liu,

1 Department of Radiology, Guangdong General Hospital, Guangdong Academy of Medical Sciences,
2 Guangzhou, China.

3 E-mail: zyliu@163.com
4

5 **Weimin Li**

6 Department of Respiratory and Critical Care Medicine, West China Hospital, Chengdu, China

7 Email: weimin003@163.com Tel: +86-02-885423998, Fax: +86-02-885313149
8

9 **Jie Tian**

10 Fellow of IAMBE, AIMBE, IEEE, SPIE, OSA, IAPR

11 Key Laboratory of Molecular Imaging, Institute of Automation, Chinese Academy of Sciences.

12 Email: jie.tian@ia.ac.cn Tel: +86-10-82618465 Fax: +86-10-62527995
13

1 **Statement of translational relevance**

2 Our study indicated that progression-free survival (PFS) of EGFR-TKI therapy in
3 stage IV *EGFR*-mutant non-small cell lung cancer (NSCLC) could be individualized
4 predicted by deep interpretation of pre-therapy CT phenotype. Clinical efficacy of
5 EGFR-TKIs could be stratified by the proposed twelve-CT-phenotypic-feature-based
6 signature, as patients in slow-progression subgroup have a better likelihood of longer
7 PFS than rapid-progression subgroup. This finding can provide support for different
8 progression subgroup patients' treatment decision. Besides, our study revealed that
9 PFS of the patients of poor signature score was not significantly longer than
10 chemotherapy-only cases. This finding provides evidence of alternative treatment
11 options for these patients to achieve better economic cost-to-benefit ratio.
12 Furthermore, we proposed an individualized prognostic model to provide PFS
13 probability recommendations for stage IV *EGFR*-mutant NSCLCs. With further
14 sufficient verification, our study might provide strong support for clinical trials and
15 drug development of EGFR-TKIs to gradually prolong the survival opportunity in
16 these patients.

17

1
2
3
4
5
6
7
8
9
10
11
12
13
14
15
16
17
18
19
20
21
22
23

Abstract

Purpose We established a computed tomography (CT)-derived approach to achieve accurate progression-free survival (PFS) prediction to EGFR tyrosine kinase inhibitors (TKIs) therapy in multicenter, stage IV *EGFR*-mutated non-small-cell lung cancer (NSCLC) patients.

Experimental Design 1032 CT-based phenotypic characteristics were extracted according to the intensity, shape and texture of NSCLC pre-therapy images. Based on these CT features extracted from 117 stage IV *EGFR*-mutant NSCLC patients, a CT-based phenotypic signature was proposed using a Cox regression model with LASSO penalty for the survival risk stratification of EGFR-TKI therapy. The signature was validated using two independent cohorts (101 and 96 patients, respectively). The benefit of EGFR-TKIs in stratified patients was then compared with another stage-IV *EGFR*-mutant NSCLC cohort only treated with standard chemotherapy (56 patients). Furthermore, an individualized prediction model incorporating the phenotypic signature and clinicopathologic risk characteristics was proposed for PFS prediction, and also validated by multicenter cohorts.

Results The signature consisted of 12 CT features demonstrated good accuracy for discriminating patients with rapid- and slow-progression to EGFR-TKI therapy in three cohorts (hazard ratio: 3.61, 3.77 and 3.67, respectively). Rapid-progression patients received EGFR TKIs did not show significant difference with patients underwent chemotherapy for progression-free survival benefit ($p = 0.682$). Decision curve analysis revealed that the proposed model significantly improved the clinical

- 1 benefit compared with the clinicopathologic-based characteristics model ($p < 0.0001$).
- 2 **Conclusion** The proposed CT-based predictive strategy can achieve individualized
- 3 prediction of PFS probability to EGFR-TKI therapy in NSCLCs, which holds promise
- 4 of improving the pre-therapy personalized management of TKIs.
- 5

1 Introduction

2 Non-small cell lung cancer (NSCLC) is the leading cause of cancer-related deaths,
 3 and its prevalence continues to increase worldwide¹. Advanced NSCLC with
 4 activating epidermal growth factor receptor (EGFR) mutations accounts for a
 5 clinically significant proportion^{2,3}. Randomized trials have consistently demonstrated
 6 that EGFR tyrosine kinase inhibitors (TKIs), such as erlotinib, gefitinib, and afatinib
 7 can promote longer progression-free survival (PFS) compared with conventional
 8 chemotherapy in this distinct subgroup of NSCLC patients⁴⁻⁸. According to the
 9 National Comprehensive Cancer Network (NCCN) those drugs are recommended as
 10 first-line therapy, but most patients eventually become resistant to them within one
 11 year after EGFR-TKI therapy⁹. Emerging Osimertinib has been recommended as
 12 second-line therapy for patients with *EGFR T790M* who have progressed on
 13 EGFR-TKI therapy such as erlotinib, gefitinib, or afatinib¹⁰. Recently intercalated
 14 regimens combining chemotherapy with TKIs were also found to extend survival^{11,12}.
 15 However, how to assess the individual patient's potential progression probability to
 16 EGFR-TKI therapy remains very challenging, and the early identification of patients
 17 with high probability of rapid encountering progression to EGFR-TKI therapy is
 18 crucial for devising appropriate treatment strategies for optimized clinical
 19 outcome^{13,14}.

20 One common hypothesis in predicting the benefit of TKIs is that the disease
 21 progression is affected by mutation types, such as exon 19 deletion and exon 21
 22 substitution of leucine for arginine in the EGFR gene^{15,16}, and clinicopathologic

1 characteristics, such as smoking status and tumor histology^{17,18}. But recent studies
 2 proved that appropriate and sufficient utilization of noninvasive diagnostic images for
 3 model-based prognostic prediction providing a new approach for survival
 4 stratification of EGFR TKIs to identify patients with different therapeutic outcomes.
 5 Imaging biomarkers based on computed tomography (CT) images, positron-emission
 6 tomography (PET) images and molecular images have been used to evaluate clinical
 7 efficacy of EGFR TKIs in NSCLC patients with EGFR mutation¹⁹⁻²². O'Connor et al.
 8 appraised various strategies to generate quantitative imaging biomarkers in the clinical
 9 development of targeted therapeutics, and revealed the effectiveness and necessity of
 10 developing such strategies for early prediction of clinical outcome^{22,23}. However,
 11 multicenter trials have not been adequately conducted to investigate the value of this
 12 technique in individualized prognostic prediction of EGFR-TKI treatment for stage IV
 13 *EGFR*-mutant NSCLC. Developing such quantitative imaging technique and testifying
 14 its validity may offer a new noninvasive and convenient approach for better
 15 understanding of the drug effect in the future development of updated EGFR TKIs, as
 16 well as for better management of therapeutic strategies for optimized patients' benefits,
 17 both clinically and economically.

18 In this study, we proposed a new approach to assess the progression probability
 19 to the recommended EGFR-TKI therapy for individual patient. Thousands of
 20 pre-therapy CT features were deeply interpreted from the patients in training cohort to
 21 select critical *EGFR*-mutation-associated phenotypic features. Then the critical
 22 features were used to develop a CT feature-based phenotypic signature for risk

stratification of PFS in multicenter stage IV *EGFR*-mutant NSCLCs. The stratified subgroups with rapid- and slow-progression to *EGFR*-TKI therapy were then compared with an independent cohort received only chemotherapy (No-TKI group) regarding to PFS. Finally, we established a new prediction model by incorporating the phenotypic signature with clinicopathologic characteristics to provide credible PFS probability recommendations of 10-month and one-year to *EGFR*-TKI therapy for individual patient. The prognostic accuracy of the proposed model was also validated in multicenter patient cohorts.

Patients and Methods

Study Design

This study was conducted in accordance with the Declaration of Helsinki. Our Institutional Review Board approved this retrospective study and waived the need for informed consent from the patients.

The entire design of this study is illustrated in Fig 1, which included the patient registration (section A), the establishment of CT phenotypic signature by using the training cohort from one hospital for risk stratification to *EGFR*-TKI therapy (sections B and C), the validation of the signature in two independent cohorts (from other two hospitals, respectively), the comparison in PFS between the stratified patient groups received TKI and the patient group received chemotherapy (section D), as well as the development and multicenter validation of the model for individualized survival prognosis prediction (sections E and F).

A. Patients

1 This multicenter retrospective study was conducted jointly by four independent
2 departments covered the eastern, western, northern, and southern of China
3 (ClinicalTrials.gov identifier: NCT02851329). All TKI cases were treated according
4 to the criteria established by NCCN.²⁴ Inclusion criteria were age 20 and older, stage
5 IV NSCLC according to the TNM classification system of the American Joint
6 Committee on Cancer,²⁵ clinically diagnosed with distant metastasis (brain, liver or
7 bone), activating *EGFR* mutations, no history of systemic anticancer therapy for
8 advanced disease, and underwent first-line or second-line EGFR-TKI therapy were
9 eligible for inclusion. Patients with history of surgery resection were excluded from
10 the study. Drugs were orally administered daily to all patients until disease progressed
11 or metastasized, with doses appropriately reduced if severe adverse events developed.
12 All eligible patients performed contrast-enhanced CT scan two weeks before
13 EGFR-TKI treatment. Clinicopathologic characteristics, such as sex, age, tumor
14 lesion location, stage at diagnosis, smoking history, performance status (PS) score,
15 intrapulmonary and distant metastases, *EGFR*-mutation subtype, and the administered
16 therapeutic regimen, were complete recorded for all eligible patients.

17 All the stage IV *EGFR*-mutant NSCLC patients in control group only received
18 chemotherapy as first-line treatment. Treating with standard care platinum-based
19 chemotherapy received pemetrexed 500 mg/m² plus cisplatin 75 mg/m² in 21-day
20 cycles till disease progression, unacceptable toxicity, or patient's refusal, as the
21 therapeutic regimen. All enrolled cases performed contrast-enhanced CT scan in two
22 weeks before chemotherapy. The choice of treatment (TKI or chemotherapy) was

made by patients voluntarily.

The follow-up interval was 4–6 weeks, and included routine laboratory tests and chest CT. Additional CT or magnetic resonance imaging was routinely performed if extrapulmonary metastasis was suspected. PFS was considered the time from the initiation of EGFR-TKI therapy to the date of confirmed disease progression or death. PFS was censored at the date of death from other causes or the date of the last follow-up visit for progression-free patients.

B. CT Image Acquisition, Interpretation, and Feature Extraction

CT scans were interpreted qualitatively and quantitatively by radiologists at each institution. Standardized reporting forms were used to record lymph node status and common sites of distant metastasis (i.e., bones, liver, and brain). Then, all multicenter CT images were gathered for tumor segmentation and feature extraction. Primary tumors of all eligible patients were manually segmented by our radiologist with more than 10 years of experience in chest CT interpretation. To ensure the reproducibility and accuracy, 50 patients were randomly selected for manual segmentation by two radiologists (reader 1 and reader 2) and the phenotypic features automatically extracted from the 50 manual segmentation results were evaluated for reproducibility analysis. These two radiologists were double-blinded for the segmentation. The inter-class correlation coefficient (ICC) was used to determine the inter-observer agreement of these features, and an ICC greater than 0.75 was considered as a mark of excellent reliability²⁶. The two radiologists were mainly responsible for delineating the boundary of each primary tumor, and all the tumors were segmented manually

1 layer-by-layer. Then reader 1 finished all the tumor segmentation. To ensure the
 2 accuracy, the segmentation results of each cohort were then evaluated by other
 3 radiologists or physicians in each center, respectively, following a guideline on image
 4 interpretation that specifically described how to define the boundary of fuzzy tumors.
 5 Appendix Part I describes the details of CT image acquisition, CT image interpretation,
 6 phenotypic feature extraction, and evaluation of consistency between different
 7 radiologists.

8 For each individual CT scan, we programmed algorithms to automatically extract
 9 phenotypic features from the manually segmented tumor region. These algorithms
 10 were partially defined by Aerts et al.'s study²⁷ and partially defined by Song et al.'s
 11 study²⁸.

12 ***C. Phenotypic Feature Selection and Signature Building***

13 The key features and their corresponding weights for prognostic prediction were
 14 screened out and calculated from the automatically extracted CT features in the
 15 training cohort by using the least absolute shrinkage and selection operator (LASSO)
 16 penalized Cox proportional hazards regression²⁹. Then, the signature was built by the
 17 weighted linear combination of all key features, and the personalized signature score
 18 can also be calculated for each patient (Appendix Part II).

19 The selected key features and the established signature were applied to stratify the
 20 training cohort into slow- and rapid-progression subgroups of *EGFR* inhibitor. This
 21 was achieved by using the X-tile plot based on Kaplan-Meier survival analyses and
 22 log-rank test³⁰. The X-tile provided the optimal binary threshold of each key feature,

as well as the signature, for risk stratification, so that different PFS behaviors in stratified subgroups can be plotted in the Kaplan-Meier survival curves. Appendix Part II describes the detailed procedures.

D. Signature Verification and Stratified EGFR-TKIs Comparison to Chemotherapy

The prognostic accuracy of the signature for patient stratification was assessed in the training cohort and another two independent validation cohorts through the time-dependent receiver operating characteristic (ROC) analyses. Both 10-months and one-year ROC curves were plotted for three cohorts, respectively, and the area under curve (AUC) was quantified.

All patients in four cohorts were stratified into rapid- and slow-progression subgroups by the proposed signature. The progression probability of the two subgroups was compared with the third group received only chemotherapy (No-TKI group). The statistical difference in PFS was analyzed to investigate the clinical benefits cross different therapies by Kaplan-Meier survival analysis and Cox regression model^{31,32}.

E. Development and Validation of an Individualized Prediction Model

Clinicopathologic characteristics (Supplementary Table S1) and the signature were assessed for their impacts on PFS by multivariable Cox regression analysis³³ to provide an easy-to-use clinical prognosis model. Reduced model selection was performed using backward stepdown analysis³⁴, and the Akaike's information criterion was applied as the stopping rule³⁵. The selected variables with significant prognostic values ($p < 0.05$) were used to develop a model for the individualized

1 probability prediction of NSCLC progression and presented as a nomogram for
 2 probability scoring of 10-month and one-year PFS.

3 The individualized prediction model was firstly developed in the training cohort,
 4 and then validated in two validation cohorts, separately. To evaluate its accuracy, the
 5 calibration curves of all three cohorts were plotted by comparing the predicted and
 6 observed progressions after bias correction in one-year PFS (Appendix Part II)³⁶.
 7 Moreover, Harrell's concordance index (C-index)³⁷ of the model was measured to
 8 quantify its discrimination performance.

9 ***F. Clinical Use***

10 To demonstrate the clinical benefits of the signature, we established another
 11 prediction nomogram model with only clinicopathologic characteristics. Then, the
 12 decision curve analysis³⁸ was performed for comparing the net benefits at different
 13 threshold probabilities given by nomograms with and without the signature.
 14 Furthermore, the net reclassification improvement (NRI) and integrated
 15 discrimination improvement (IDI) were also quantified³⁹ for evaluating the extra
 16 benefits of the signature.

17 ***Statistical Analysis***

18 Statistical analysis was conducted using R software (version 3.2.3,
 19 <http://www.Rproject.org>). Parameters of the packages in R used in this study were
 20 described in Appendix Part III. The reported statistical significance levels were all
 21 two-sided, and p values < 0.05 were considered to indicate significance.

22 **Results**

A. Patients

Treatment

370 patients with stage IV *EGFR*-mutant NSCLC from four independent departments were enrolled according to our criteria. Among these, 314 cases received TKIs (117 cases, 101 cases, and 96 cases in three cohorts, respectively), and 56 cases from two independent departments received standard chemotherapy were eligible to consist as the comparison group. Supplementary Table S2 describes the detail of drugs, patients, and enrollment time. Notably, the administration time of TKI drugs and the discontinuation cases in the cohorts were not significantly different ($p > 0.5$).

Clinicopathologic characteristics

Clinicopathologic characteristics of the *EGFR*-TKI treatment cohorts and chemotherapy cohort are presented in Table 1. In the three TKI treatment cohorts, 300 of 314 (96%) patients suffered NSCLC progression during the follow-up period, median follow-up period is 12.2 months, 13.5 months and 11.8 months, respectively. There was no significant difference in PFS among them (median PFS: training cohort, 8.1 months; validation cohort 1, 9.2 months; validation cohort 2, 8.2 months; Kruskal-Wallis H test, $p = 0.205$). Furthermore, there were no significant differences ($p > 0.2$ in following categories) in PFS regarding to age, smoking status, pulmonary metastases, brain metastases, bone metastases, and liver metastases among all three cohorts neither.

56 eligible patients were included in the comparison group from two different hospitals (37 cases and 19 cases, respectively). Mean time of treatment was not

significantly different between them ($p = 0.562$), and only one case of treatment discontinuation occurred. Median PFS of the chemotherapy group was 4.5 months.

B. CT Image and Phenotypic Feature

Phenotype feature extraction was performed on the CT images which acquired within two weeks before treatment for each patient. The inter-observer reproducibility of CT features extraction was satisfactory. ICC reached 0.872 to 0.935 for the two radiologists. For each individual CT scan, we managed to extract 1032 phenotypic features from the manually segmented tumor region, in which 440 features from the study of Aerts and the other 592 features proposed by the study of Song. Then, more than 120 thousand features were obtained from the segmented CT data in the training cohort. After that, 12 key features were screened out using the LASSO Cox regression model. They and their cut-off for patients' risk stratification are listed in Supplementary Table S3.

C. Feature Selection and Signature Building

The weights of 12 selected key features for signature building were calculated by the LASSO Cox regression model on the basis of the training cohort, and the signature calculation equation is given in the Appendix Part II. Cut-off value of the signature is -1.15 by X-tile. The X-tile plots of the 12 key features are shown in the Supplementary Fig S1, which revealed their impacts on the prognostic stratification in the training cohort.

D. Signature Verification and Stratified EGFR-TKIs Comparison to Chemotherapy

The signature score of each individual patient is plotted in left panels of Fig 2A

(training cohort), B (validation cohort 1), and C (validation cohort 2), and all three cohorts consistently indicated that there were more slow-progression patients (red bars) than rapid-progression patients (blue bars) in the expectation of *EGFR* inhibitor. The ratio of rapid-progression patients in each cohort was 36%, 35%, and 33%, respectively. The Kaplan-Meier survival curves confirmed the significant difference in PFS between the stratified rapid- and slow-progression subgroups in all cohorts (middle panels of Fig 2A, B, and C, $p < 0.0001$ in all cohorts). Hazard ratio (HR) reached over 3.6 in all cohorts, which suggested the dramatic difference of the two subgroup's PFS in EGFR-TKI therapies. AUC of the time-dependent ROC curves (right panels of Fig 2A, B, and C) ranged from 0.711 to 0.738 for 10-month PFS, and 0.701 to 0.822 for one-year PFS in three cohorts. This proved the discrimination accuracy of PFS was consistently high for using the signature.

In the comparison between stratified subgroups with TKIs and the independent group with chemotherapy (No-TKI group), the Kaplan-Meier survival curves (Fig 3) demonstrated that the rapid-progression subgroup (110 patients, median PFS: 5.6 months, interquartile range (IQR): 2.9 to 7.8 months) is overlapped with no-TKI group (median PFS: 4.5 months, IQR: 2.3 to 7.2 months). No significant PFS difference was found between them ($p = 0.682$, HR: 1.02, 95%CI: 0.743-1.425), but they were both significantly different from the slow-progression subgroup (204 patients, median PFS: 10.7 months, IQR: 7.7 to 17.9 months, $p < 0.0001$, HR: 3.52, 95%CI: 2.50-4.65). An extra experiment was done to apply the signature to the chemotherapy cases for risk stratification, and no significant difference in PFS was

found between the two chemotherapy groups ($p > 0.05$, Supplementary Fig S5). This revealed that the signature can effectively identify the patient with high risk of rapid progression, and for these patients, EGFR TKI showed no better clinical benefits than conventional chemotherapy did.

E. Development and Validation of an Individualized Model

The multivariable Cox analysis in the training cohort identified two clinicopathologic characteristics (N category and smoking status, both $p < 0.05$) and the signature ($p < 0.0001$) as independent variables with significant prognostic value (Table 2). Then, an individualized progression probability prediction model incorporating all these variables was established and presented as a nomogram (Fig 4A).

The calibration curves obtained from the individualized nomogram showed good agreements between prediction and observation of the one-year NSCLC progression probability in the training and two independent validation cohorts (Fig 4B). The Harrell's C-index of the nomogram was 0.743, 95% CI: 0.700 to 0.786 for the training cohort, as well as 0.718, 95% CI: 0.669 to 0.767 and 0.720, 95% CI: 0.676 to 0.764 for the validation cohorts, respectively.

If we removed the signature from the nomogram and kept only significant clinicopathologic variables, the C-index dropped to 0.633 (95% CI: 0.584-0.682), 0.622 (95% CI: 0.570-0.674), and 0.630 (95% CI: 0.578-0.682) in three cohorts. The integration of the CT-based signature into the nomogram improved the prediction accuracy significantly regarding to NRI (0.503, 95% CI: 0.260 to 0.604, $p < 0.0001$) and IDI (0.161, 90% CI: 0.080 to 0.248, $p < 0.0001$).

1 ***F. Clinical Use***

2 The decision curve analysis for the individualized nomogram with and without
 3 integrating the signature is shown in Fig 4C. It demonstrated that the nomogram with
 4 signature provided the largest overall net benefit in predicting PFS with EGFR TKIs
 5 comparing with the nomogram without it, the treat-all-patients scheme, and the
 6 treat-none scheme, if the threshold probability of a patient is $> 7\%$.

7 **Discussion**

8 Although there are new treatment strategies for patients who have progressed on
 9 sensitizing EGFR-TKI therapy, erlotinib, gefitinib, and afatinib are still recommended
 10 first-line treatments for NSCLC patients^{10,40}. Disease progression is the common
 11 reason to stop EGFR-TKI therapy according to NCCN, but how to assess when the
 12 progression happens for individual patient is great challenging^{41,42}. Our study
 13 proposed a noninvasive approach to this clinical problem. We established a CT
 14 feature-based signature for survival risk stratification to EGFR-TKI therapy in stage
 15 IV *EGFR*-mutant NSCLC patients. Then, we integrated the signature with clinical
 16 characteristics (N category and smoking status) to develop a pre-therapy model for
 17 individualized probability prediction of TKI progression in these patients. Both
 18 signature and nomogram were validated through multicenter patient cohorts resulting
 19 in adequate accuracy in EGFR TKI progression discrimination and prediction. To the
 20 best of our knowledge, this is the first multicenter retrospective study that
 21 comprehensively proved the significant prognostic value of the CT signature in stage
 22 IV *EGFR*-mutant NSCLC patients with EGFR-TKI therapy.

1 The signature demonstrated that about 35% patients were predicted with
 2 rapid-progression of EGFR inhibitor by the signature, and indeed showed 48% less
 3 PFS benefit than slow-progression subgroups through multicenter cohorts. HR over
 4 3.6 in all cohorts also indicated the dramatic difference on PFS between the rapid- and
 5 slow-progression subgroups stratified by quantitatively interpreting pre-therapy CT
 6 images. Consistent with previous randomized trials^{4,6,7} and meta-analysis⁸,
 7 EGFR-TKI therapy showed an overall longer PFS compared with chemotherapy in
 8 our multicenter study. Surprisingly, our study revealed that the *EGFR*-mutant
 9 NSCLCs with poor signature score (rapid-progression subgroup) did not have
 10 significantly longer PFS after EGFR TKIs than the chemotherapy (p = 0.682).
 11 Therefore, for these rapid-progression patients, their treatment programs and
 12 follow-up should be developed more rigorous.

13 The multivariable Cox analysis identified two clinicopathologic characteristics
 14 (N category, and smoking status), as well as the signature as independent risk factors
 15 for the prediction of PFS to EGFR-TKI therapy. Lymph node metastases and smoking
 16 are widely recognized prognostic characteristics for NSCLC^{16,43-46}, whereas *EGFR*
 17 mutation (exon 19 deletion or exon 21 L858R substitution) subtype is still a
 18 controversial prognostic factor in different trials^{15,44,45,47}. Here, we found no
 19 difference between the two common mutations for the benefit of EGFR TKIs (p >
 20 0.05). Besides, the analysis did not show significant prognostic impact regarding to
 21 gender, and this factor needs to be further validated¹⁶. The possible reasons of the
 22 inconsistency might be that the eligible patients were enrolled from different

1 ethnicities and/or different countries. In addition, T3 is the only significant category
 2 compared with T1, therefore T stage is not suitable to be included as an independent
 3 factor into the model in this study. Furthermore, studies from the perspective of
 4 biological mechanism to explain why phenotypic characteristics reveal treatment
 5 outcomes are rare. Larger scale of patient populations is still needed for identifying
 6 potential clinical risk factors, and physiological explanations of the prognostic tumor
 7 phenotype. However, this did not compromise the effectiveness and robustness of our
 8 proposed signature for prognostic prediction.

9 To further investigate that how much extra benefit we can obtain for
 10 individualized prediction on PFS by incorporating the signature, we developed and
 11 compared new prediction nomograms incorporating clinicopathologic risk factors
 12 with and without the signature. Then, the discrimination of the no-signature
 13 nomogram yielded significant reduction in all cohorts (C-index, no-signature vs.
 14 signature nomogram, training cohort: 0.743 vs. 0.633; validation cohort 1: 0.718 vs.
 15 0.622; validation cohort 2: 0.720 vs. 0.630; all comparisons $p < 0.001$).

16 There is a general concern of utilizing a CT feature-based model for multicenter
 17 applications because of the high heterogeneity in CT image acquisition in different
 18 institutions (different system manufacturers, acquisition settings, and tomographic
 19 reconstruction methods)^{28,48-50}. However, our study demonstrated that the signature
 20 and signature-based model established from one institutional data were remarkably
 21 robust for progression stratification and prediction in other institutions. The
 22 multicenter application was very direct, without any adjustment of key features and

1 their corresponding weights for signature building, yet all quantitative evaluations
 2 yielded high consistency cross all multicenter cohorts. Once we mixed all patient data
 3 for NRI and IDI calculation, as well as decision curve analysis, they all proved that
 4 the nomogram with signature offered significant improvement (NRI, 0.503, $p <$
 5 0.0001; IDI, 0.161, $p < 0.0001$) for individualized PFS prediction comparing with the
 6 nomogram without it.

7 Our study has several important clinical and research implications. The signature
 8 and the integrated nomogram showed valuable prognostic and predictive potential to
 9 EGFR-TKI therapy. Therefore, it will be useful for counseling patients, directing
 10 personalized therapeutic regimen management, as well as achieving better economic
 11 cost-to-benefit ratio for different stratified subgroups. With further sufficient
 12 validation, they might be important as independent predictors for future clinical trials
 13 and drug development of EGFR TKIs to gradually prolong the survival opportunity in
 14 these patients.

15 In conclusion, the proposed prognostic strategy can achieve effective and robust
 16 prognostic stratification and individualized prediction of PFS to EGFR TKIs in
 17 NSCLCs, which holds promise of improving the pre-therapy personalized
 18 management of EGFR TKIs for stage IV *EGFR*-mutant NSCLCs.

19
 20

REFERENCES

1. Siegel RL, Miller KD, Jemal A. Cancer statistics, 2016. *CA Cancer J Clin*. 2016;66:7–30.
2. Jia Y, Yun C-H, Park E, Ercan D, Manuia M, Juarez J, et al. Overcoming EGFR(T790M) and EGFR(C797S) resistance with mutant-selective allosteric inhibitors. *Nature*. 2016;534:129–32.
3. Gainor JF, Varghese AM, Ou SHI, Kabraji S, Awad MM, Katayama R, et al. ALK rearrangements are mutually exclusive with mutations in EGFR or KRAS: An analysis of 1,683 patients with non-small cell lung cancer. *Clin Cancer Res*. 2013;19:4273–81.
4. Lee SM, Lewanski CR, Counsell N, Ottensmeier C, Bates A, Patel N, et al. Randomized trial of erlotinib plus whole-brain radiotherapy for NSCLC patients with multiple brain metastases. *J Natl Cancer Inst*. 2014;106.
5. Novello S. Epidermal growth factor receptor tyrosine kinase inhibitors as adjuvant therapy in completely resected non-small-cell lung cancer. *J Clin Oncol*. 2015;33:3985–6.
6. Soria J, Wu Y, Nakagawa K, Kim S, Yang J, Ahn M, et al. Gefitinib plus chemotherapy versus placebo plus chemotherapy in EGFR -mutation-positive non-small-cell lung cancer after progression on first-line gefitinib (IMPRESS): a phase 3 randomised trial. *Lancet Oncol*. Elsevier Ltd; 2015;2045:1–9.
7. Sequist L V, Yang JC-H, Yamamoto N, O’Byrne K, Hirsh V, Mok T, et al. Phase III study of afatinib or cisplatin plus pemetrexed in patients with metastatic lung adenocarcinoma with EGFR mutations. *J Clin Oncol*. 2013;31:3327–34.
8. Gao G, Ren S, Li A, Xu J, Xu Q, Su C, et al. Epidermal growth factor receptor-tyrosine kinase inhibitor therapy is effective as first-line treatment of advanced non-small-cell lung

- 1 cancer with mutated EGFR: A meta-analysis from six phase III randomized controlled trials.
2 Int J Cancer. 2012;131:822–9.
- 3 9. Yu HA, Arcila ME, Rekhtman N, Sima CS, Zakowski MF, Pao W, et al. Analysis of tumor
4 specimens at the time of acquired resistance to EGFR-TKI therapy in 155 patients with
5 EGFR-mutant lung cancers. Clin Cancer Res. 2013;19:2240–7.
- 6 10. Mok TS, Wu Y-L, Ahn M-J, Garassino MC, Kim HR, Ramalingam SS, et al. Osimertinib or
7 Platinum–Pemetrexed in *EGFR* T790M–Positive Lung Cancer. N Engl J Med. 2017;376:629–
8 40.
- 9 11. Wu Y-L, Lee JS, Thongprasert S, Yu C-J, Zhang L, Ladrera G, et al. Intercalated combination
10 of chemotherapy and erlotinib for patients with advanced stage non-small-cell lung cancer
11 (FASTACT-2): a randomised, double-blind trial. Lancet Oncol. 2013;14:777–86.
- 12 12. Seto T, Kato T, Nishio M, Goto K, Atagi S, Hosomi Y, et al. Erlotinib alone or with
13 bevacizumab as first-line therapy in patients with advanced non-squamous non-small-cell
14 lung cancer harbouring EGFR mutations (JO25567): An open-label, randomised, multicentre,
15 phase 2 study. Lancet Oncol. 2014;15:1236–44.
- 16 13. Crystal AS, Shaw AT, Sequist L V, Friboulet L, Niederst MJ, Lockerman EL, et al.
17 Patient-derived models of acquired resistance can identify effective drug combinations for
18 cancer. Science. 2014;346:1480–6.
- 19 14. Taguchi F, Solomon B, Gregorc V, Roder H, Gray R, Kasahara K, et al. Mass spectrometry to
20 classify non-small-cell lung cancer patients for clinical outcome after treatment with
21 epidermal growth factor receptor tyrosine kinase inhibitors: a multicohort cross-institutional
22 study. J Natl Cancer Inst. 2007;99:838–46.

- 1 15. Wu YL, Zhou C, Hu CP, Feng J, Lu S, Huang Y, et al. Afatinib versus cisplatin plus
2 gemcitabine for first-line treatment of Asian patients with advanced non-small-cell lung
3 cancer harbouring EGFR mutations (LUX-Lung 6): An open-label, randomised phase 3 trial.
4 *Lancet Oncol.* 2014;15:213–22.
- 5 16. Wu YL, Zhou C, Liang CK, Wu G, Liu X, Zhong Z, et al. First-line erlotinib versus
6 gemcitabine/cisplatin in patients with advanced EGFR mutation-positive non-small-cell lung
7 cancer: Analyses from the phase III, randomized, open-label, ENSURE study. *Ann Oncol.*
8 2015;26:1883–9.
- 9 17. Shepherd FA, Rodrigues Pereira J, Ciuleanu T, Tan EH, Hirsh V, Thongprasert S, et al.
10 Erlotinib in previously treated non-small-cell lung cancer. *N Engl J Med.* 2005;353:123–32.
- 11 18. Ho GYF, Zheng SQL, Cushman M, Perez-Soler R, Kim M, Xue XN, et al. Associations of
12 Insulin and IGFBP-3 with Lung Cancer Susceptibility in Current Smokers. *J Natl Cancer*
13 *I* 2016;108(7).
- 14 19. Dingemans AMC, de langheer AJ, van den Boogaart V, Marcus JT, Backes WH, Scholtens
15 HTGM, et al. First-line erlotinib and bevacizumab in patients with locally advanced and/or
16 metastatic non-small-cell lung cancer: A phase II study including molecular imaging. *Ann*
17 *Oncol.* 2011;22:559–66.
- 18 20. Dai D, Li X-F, Wang J, Liu J-J, Zhu Y-J, Zhang Y, et al. Predictive efficacy of
19 C-PD153035 PET imaging for EGFR-tyrosine kinase inhibitor sensitivity in non-small cell
20 lung cancer patients. *Int J Cancer.* 2016;138:1003–12.

21. Nishino M, Dahlberg SE, Cardarella S, Jackman DM, Rabin MS, Hatabu H, et al. Tumor volume decrease at 8 weeks is associated with longer survival in EGFR-mutant advanced non-small-cell lung cancer patients treated with EGFR TKI. *J Thorac Oncol.* 2013;8:1059–68.
22. O'Connor JPB, Jackson A, Asselin M-C, Buckley DL, Parker GJM, Jayson GC. Quantitative imaging biomarkers in the clinical development of targeted therapeutics: current and future perspectives. *Lancet Oncol.* 2008;9:766–76.
23. O'Connor J, Aboagye E, Adams J, Aerts H, Barrington S, Beer A. Imaging biomarker roadmap for cancer studies. *Nat Rev Clin Oncol.* 2017;14:169–86.
24. Ettinger DS, Wood DE, Akerley W, Bazhenova LA, Borghaei H, Camidge DR, et al. NCCN Guidelines Insights: Non-Small Cell Lung Cancer, Version 4.2016. *J Natl Compr Canc Netw.* 2016;14:255–64.
25. Edge, S., Byrd, D.R., Compton, C.C., Fritz, A.G., Greene, F.L., Trotti A. *AJCC Cancer Staging Manual* | Stephen Edge | Springer. Springer. 2009.
26. Barry WT, Kernagis DN, Dressman HK, Griffis RJ, Hunter JD, Olson JA, et al. Intratumor heterogeneity and precision of microarray-based predictors of breast cancer biology and clinical outcome. *J Clin Oncol.* 2010;28:2198–206.
27. Aerts HJWL, Velazquez ER, Leijenaar RTH, Parmar C, Grossmann P, Cavalho S, et al. Decoding tumour phenotype by noninvasive imaging using a quantitative radiomics approach. *Nat Commun.* 2014;5:4006.
28. Song J, Liu Z, Zhong W, Huang Y, Ma Z, Dong D, et al. Non-small cell lung cancer: quantitative phenotypic analysis of CT images as a potential marker of prognosis. *Sci Rep.* Nature Publishing Group; 2016;6:38282.

- 1 29. Pellagatti A, Benner A, Mills KI, Cazzola M, Giagounidis A, Perry J, et al. Identification of
2 gene expression-based prognostic markers in the hematopoietic stem cells of patients with
3 myelodysplastic syndromes. *J Clin Oncol*. 2013;31:3557–64.
- 4 30. Stish BJ, Pisansky TM, Harmsen WS, Davis BJ, Tzou KS, Choo R, et al. Improved
5 metastasis-free and survival outcomes with early salvage radiotherapy in men with detectable
6 prostate-specific antigen after prostatectomy for prostate cancer. *J Clin Oncol*. 2016;34:3864–
7 71.
- 8 31. Dignam, James J.; Zhang, Qiang; Kocherginsky MN. The Use and Interpretation of
9 Competing Risks Regression Models. *Clin Cancer Res*. 2012;18:2301–8.
- 10 32. Shukla S, Evans JR, Malik R, Feng FY, Dhanasekaran SM, Cao X, et al. Development of a
11 RNA-Seq Based Prognostic Signature in Lung Adenocarcinoma. *J Natl Cancer Inst*.
12 2017;109.
- 13 33. Verhelst X, Vanderschaeghe D, Castéra L, Raes T, Geerts A, Francoz C, et al. A
14 glycomics-based test predicts the development of hepatocellular carcinoma in cirrhosis. *Clin*
15 *Cancer Res*. 2017;23:2750–8.
- 16 34. Yates DR, Hupertan V, Colin P, Ouzzane A, Descazeaud A, Long JA, et al. Cancer-specific
17 survival after radical nephroureterectomy for upper urinary tract urothelial carcinoma:
18 proposal and multi-institutional validation of a post-operative nomogram. *Brit J Cancer*
19 2012;106(6):1083-8.
- 20 35. Mittendorf EA, Jeruss JS, Tucker SL, Kolli A, Newman LA, Gonzalez-Angulo AM, et al.
21 Validation of a novel staging system for disease-specific survival in patients with breast
22 cancer treated with neoadjuvant chemotherapy. *J Clin Oncol*. 2011;29:1956–62.

- 1 36. Han JY, Park K, Kim SW, Lee DH, Kim HY, Kim HT, et al. First-SIGNAL: First-line
2 single-agent iressa versus gemcitabine and cisplatin trial in never-smokers with
3 adenocarcinoma of the lung. *J Clin Oncol.* 2012;30:1122–8.
- 4 37. Ueno H, Mochizuki H, Akagi Y, Kusumi T, Yamada K, Ikegami M, et al. Optimal colorectal
5 cancer staging criteria in TNM classification. *J Clin Oncol.* 2012;30:1519–26.
- 6 38. Vickers AJ, Elkin EB. Decision curve analysis: a novel method for evaluating prediction
7 models. *Med Decis Mak.* 2006;26:565–74.
- 8 39. Tangri N, Stevens L a, Griffith J, Tighiouart H, Djurdjev O, Naimark D, et al. A predictive
9 model for progression of chronic kidney disease to kidney failure. *JAMA.* 2011;305:1553–9.
- 10 40. Jänne P a, Yang JC-H, Kim D-W, Planchard D, Ohe Y, Ramalingam SS, et al. AZD9291 in
11 EGFR Inhibitor-Resistant Non-Small-Cell Lung Cancer. *N Engl J Med.* 2015;372:1689–99.
- 12 41. Riely GJ, Yu HA. EGFR: The paradigm of an oncogene-driven lung cancer. *Clin Cancer Res.*
13 2015;21:2221–6.
- 14 42. Kosaka T, Yatabe Y, Endoh H, Yoshida K, Hida T, Tsuboi M, et al. Analysis of epidermal
15 growth factor receptor gene mutation in patients with non-small cell lung cancer and acquired
16 resistance to gefitinib. *Clin Cancer Res.* 2006;12:5764–9.
- 17 43. Masters GA, Temin S, Azzoli CG, Giaccone G, Baker S, Brahmer JR, et al. Systemic Therapy
18 for Stage IV Non-Small-Cell Lung Cancer: American Society of Clinical Oncology Clinical
19 Practice Guideline Update. *J Clin Oncol.* 2015;33:JCO.2015.62.1342 – .
- 20 44. Inoue a, Kobayashi K, Maemondo M, Sugawara S, Oizumi S, Isobe H, et al. Updated overall
21 survival results from a randomized phase III trial comparing gefitinib with

- 1 carboplatin-paclitaxel for chemo-naïve non-small cell lung cancer with sensitive EGFR gene
- 2 mutations (NEJ002). *Ann Oncol.* 2013;24:54–9.
- 3 45. Zhou C, Wu YL, Chen G, Feng J, Liu XQ, Wang C, et al. Erlotinib versus chemotherapy as
- 4 first-line treatment for patients with advanced EGFR mutation-positive non-small-cell lung
- 5 cancer (OPTIMAL, CTONG-0802): a multicentre, open-label, randomised, phase 3 study.
- 6 *Lancet Oncol.* 2011;12:735–42.
- 7 46. Liang W, Zhang L, Jiang G, Wang Q, Liu L, Liu D, et al. Development and Validation of a
- 8 Nomogram for Predicting Survival in Patients With Resected Non-Small-Cell Lung Cancer. *J*
- 9 *Clin Oncol.* 2015;33:861–9.
- 10 47. Maemondo M, Inoue A, Kobayashi K, Sugawara S, Oizumi S, Isobe H, et al. Gefitinib or
- 11 chemotherapy for non-small-cell lung cancer with mutated EGFR. *N Engl J Med.*
- 12 2010;362:2380–8.
- 13 48. Meignan M, Cottreau AS, Versari A, Chartier L, Dupuis J, Boussetta S, et al. Baseline
- 14 metabolic tumor volume predicts outcome in high-tumor-burden follicular lymphoma: A
- 15 pooled analysis of three multicenter studies. *J Clin Oncol.* 2016. page 3618–26.
- 16 49. Hulbert A, Jusue Torres I, Stark A, Chen C, Rodgers K, Lee B, et al. Early Detection of Lung
- 17 Cancer using DNA Promoter Hypermethylation in Plasma and Sputum. *Clin Cancer Res.*
- 18 2016;23:1998–2006.
- 19 50. Zhang B, Tian J, Dong D, Gu D, Dong Y, Zhang L, et al. Radiomics of Multi-parametric MRI
- 20 for Pretreatment Prediction of Progression-Free Survival in Advanced Nasopharyngeal
- 21 Carcinoma, *Clinical Cancer Research.* 2017.

Table 1. Demographic and clinicopathologic characteristics of the training cohort and two independent validation cohorts. Slow and Rapid represents the slow-progression and rapid-progression subgroups by the signature, respectively. PFS: progression-free survival (months); PS: performance status.

Demographic or Clinicopathologic Characteristic	Training Set (N = 117)				Independent Validation Set 1 (N = 101)				Independent Validation Set 2 (N = 96)				No-TKI (N = 56)	
	No.	Median PFS	Slow (%)	Rapid (%)	No.	Median PFS	Slow (%)	Rapid (%)	No.	Median PFS	Slow (%)	Rapid (%)	No.	Median PFS
Gender														
Male	44	7.7	33 (75%)	11 (25%)	41	10.0	25 (61%)	16 (39%)	41	7.1	22 (54%)	19 (46%)	30	4.6
Female	73	8.2	42 (58%)	31 (42%)	60	9.5	40 (67%)	20 (33%)	55	8.4	42 (76%)	13 (24%)	26	4.5
Age, years														
≤ 65	67	7.7	40 (60%)	27 (40%)	66	10.0	47 (71%)	19 (29%)	66	7.8	43 (44%)	23 (56%)	43	5.1
> 65	50	8.0	35 (70%)	15 (30%)	35	10.0	18 (51%)	17 (49%)	30	8.4	21 (32%)	9 (68%)	13	4.1
Tumor location														
Right	69	7.2	47 (67%)	22 (33%)	55	9.6	36 (66%)	19 (34%)	45	7.8	22 (65%)	23 (35%)	23	4.6
Other	48	8.5	28 (58%)	20 (42%)	46	10.2	29 (63%)	17 (37%)	51	7.2	42 (81%)	9 (18%)	33	4.3
Pathologic T stage														
T1	25	11.0	21 (84%)	4 (16%)	24	10.1	18 (75%)	6 (25%)	8	8.4	6 (75%)	2 (25%)	6	5.3
T2	27	8.8	19 (70%)	8 (30%)	20	10.0	16 (80%)	4 (20%)	40	8.3	32 (80%)	8 (20%)	15	4.2
T3	18	7.5	12 (67%)	6 (33%)	13	6.9	2 (16%)	11 (84%)	15	6.9	8 (53%)	7 (47%)	21	4.0
T4	47	7.6	23 (49%)	24 (51%)	44	8.0	29 (66%)	15 (34%)	33	7.2	18 (55%)	15 (45%)	14	3.8
Pathologic N stage														
N0	29	10.0	21 (74%)	8 (26%)	20	10.5	17 (85%)	3 (15%)	28	9.3	22 (79%)	6 (21%)	5	5.8
N1	11	10.5	8 (73%)	3 (27%)	7	10.1	5 (71%)	2 (29%)	10	6.9	5 (50%)	5 (50%)	20	4.1
N2	50	8.1	31 (62%)	19 (38%)	42	9.7	27 (64%)	15 (36%)	31	8.3	22 (71%)	9 (29%)	11	5.0
N3	27	6.9	15 (56%)	12 (44%)	32	8.1	16 (50%)	16 (50%)	27	6.0	15 (56%)	12 (44%)	20	4.1
Tobacco use														
Smoker	53	7.4	29 (55%)	24 (45%)	21	10.0	8 (38%)	13 (62%)	17	7.1	11 (65%)	6 (35%)	14	3.4
No smoker	64	8.9	46 (72%)	18 (28%)	80	9.8	57 (71%)	23 (29%)	79	8.3	53 (67%)	26 (33%)	42	5.4
Base PS Score														
≥ 2	80	7.7	52 (65%)	28 (35%)	68	9.5	37 (54%)	31 (46%)	62	8.2	32 (52%)	30 (48%)	43	4.0
< 2	37	9.5	23 (62%)	14 (38%)	33	12.5	28 (85%)	5 (15%)	34	7.8	32 (94%)	2 (6%)	13	5.2
Brain metastasis														
Yes	39	7.2	22 (57%)	17 (43%)	37	10.1	23 (62%)	14 (38%)	19	6.2	11 (58%)	8 (42%)	20	4.8
No	78	8.1	53 (68%)	25 (32%)	64	10.5	42 (66%)	22 (34%)	77	8.4	53 (69%)	24 (31%)	36	4.0
Bone metastasis														
Yes	51	7.6	30 (59%)	21 (41%)	44	9.2	28 (64%)	16 (36%)	32	7.5	18 (56%)	14 (44%)	23	5.0
No	66	8.4	45 (68%)	21 (32%)	57	10.7	37 (64%)	20 (36%)	64	8.3	46 (72%)	18 (28%)	33	4.2
Liver metastasis														
Yes	10	8.0	6 (60%)	4 (40%)	12	9.7	7 (58%)	5 (42%)	12	7.4	8 (67%)	4 (33%)	9	4.3
No	107	7.7	69 (64%)	38 (36%)	89	10.2	58 (65%)	31 (35%)	84	8.4	56 (67%)	28 (33%)	47	4.3
Lung metastasis														
Yes	56	7.8	32 (57%)	24 (43%)	54	10.2	34 (63%)	20 (37%)	47	7.1	28 (60%)	19 (40%)	33	4.6
No	61	7.7	43 (70%)	18 (30%)	47	9.5	31 (66%)	16 (34%)	49	8.4	36 (74%)	13 (26%)	23	4.2
Mutation status:														
EGFR 19Del	57	8.4	38 (67%)	19 (33%)	60	11.0	40 (33%)	20 (67%)	41	8.4	28 (68%)	13 (32%)	21	4.6
EGFR 21L858R	49	7.7	30 (61%)	19 (39%)	35	10.5	21 (60%)	14 (40%)	48	7.9	29 (60%)	19 (40%)	30	4.2
Other EGFR	11	6.7	7 (64%)	4 (36%)	6	10.0	4 (67%)	2 (33%)	7	7.2	7 (100%)	0 (0%)	5	3.8
Line of treatment														
First line	79	7.7	46 (58%)	33 (42%)	67	10.4	41 (61%)	26 (39%)	69	8.0	45 (65%)	24 (35%)	-	-
Second line	38	9.5	29 (76%)	9 (24%)	34	10.1	24 (71%)	10 (29%)	27	8.4	19 (70%)	8 (30%)	-	-

Table 2. The signature and two clinicopathological characteristics which incorporated into the individualized prognostic model. HR: hazard ratio; CI: confidence interval.

Variables	Model		
	β	HR (95%CI)	P value
Pathological N category N0 as reference			
Pathological N1 category	0.14	1.16 (1.10, 2.89)	0.028
Pathological N2 category	0.78	2.20 (1.28, 3.78)	0.016
Pathological N3 category	1.06	2.90 (1.60, 5.25)	0.005
Smoke	1.00	2.73 (1.38, 4.42)	0.002
Twelve-feature-based signature	1.65	5.18 (3.24, 8.26)	<0.0001

3
4

Figure legends

Figure 1. The flowchart of this study. Including the patient registration (section A in the “Patients and Methods”), the establishment of CT phenotypic signature by using training cohort for risk stratification in developing EGFR inhibitor resistance (sections B and C), the validation of the signature in two independent cohorts, the comparison in PFS between stratified patient groups with TKIs and the patient group with chemotherapy (section D), as well as the development and multicenter validation of the nomogram model for individualized prognosis prediction (sections E and F).

Figure 2. Risk score according to the twelve-feature-based signature (left), Kaplan-Meier survival (middle), and time-dependent ROC curves (right) in the training and independent validation sets. Data are based on the AUC (95% CI) or HR (95% CI). (A), (B) and (C) represent the training cohort and two independent validation cohorts, respectively. All scores have subtracted the cut-off. AUCs at 10-months and one-year progression-free survival were determined to assess prognostic accuracy, and p values were calculated using the log-rank test. AUC = area under the curve; CI = confidence interval; HR = hazards ratio; ROC = receiver operator characteristic.

Figure 3. Progression probability of three different patient cohorts. The blue line represents slow-progression subgroup patients, the red line represents rapid-progression subgroup patients, and the green line represents the patients treated with chemotherapy. The slow-progression patients with longer survival compared with the rapid-progression patients ($p < 0.0001$), and the patients treated with chemotherapy (no-TKI, $p < 0.0001$). We find that, for these rapid-progression patients, EGFR TKIs showed no better clinical benefits than conventional chemotherapy did ($p = 0.682$).

Figure 4: Nomogram to predict risk of disease progression of stage IV *EGFR*-mutant NSCLC patients received *EGFR* TKIs. (A) represents the nomogram for predicting the probability of patients with 10-month and one-year PFS after *EGFR* TKI treatment. (B) plots depict the calibration of the nomogram in terms of agreement between predicted and observed one-year PFS. Performances of the training set and validation sets are shown on the plot relative to the 45-degree line, which represents perfect prediction. (C) decision curve analysis for the comparison of prognostic model with (red line) and without (blue line) integrating the signature. The y-axis measures the net benefit. The net benefit was calculated by subtracting the proportion of all patients who are false positive from the proportion who are true positive, weighting by the relative harm of forgoing treatment compared with the negative consequences of an unnecessary treatment. *EGFR* = epidermal growth factor receptor; PFS = progression-free survival; PS = performance status; TKI = tyrosine kinase inhibitor.

Figure 1

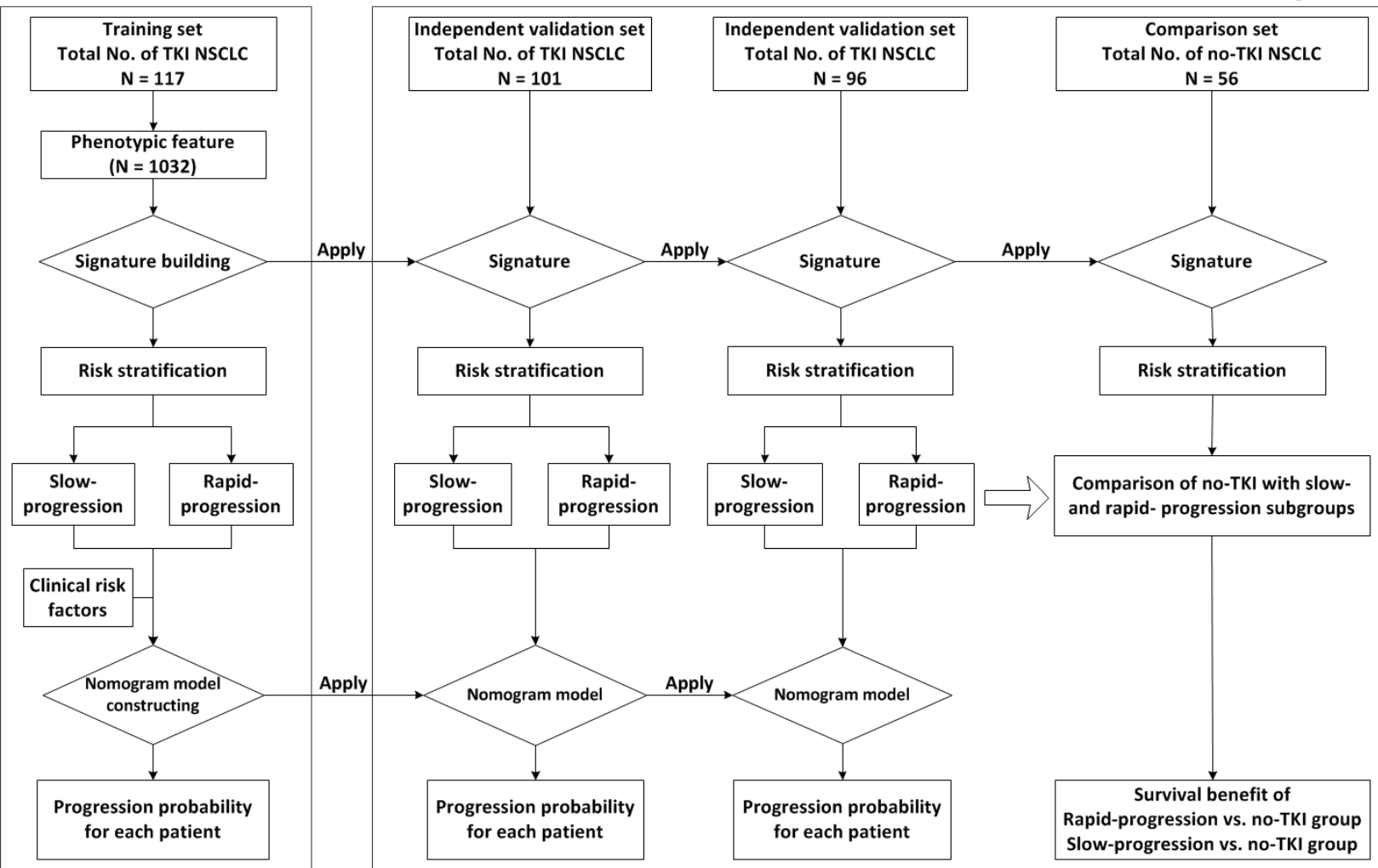


Figure 2

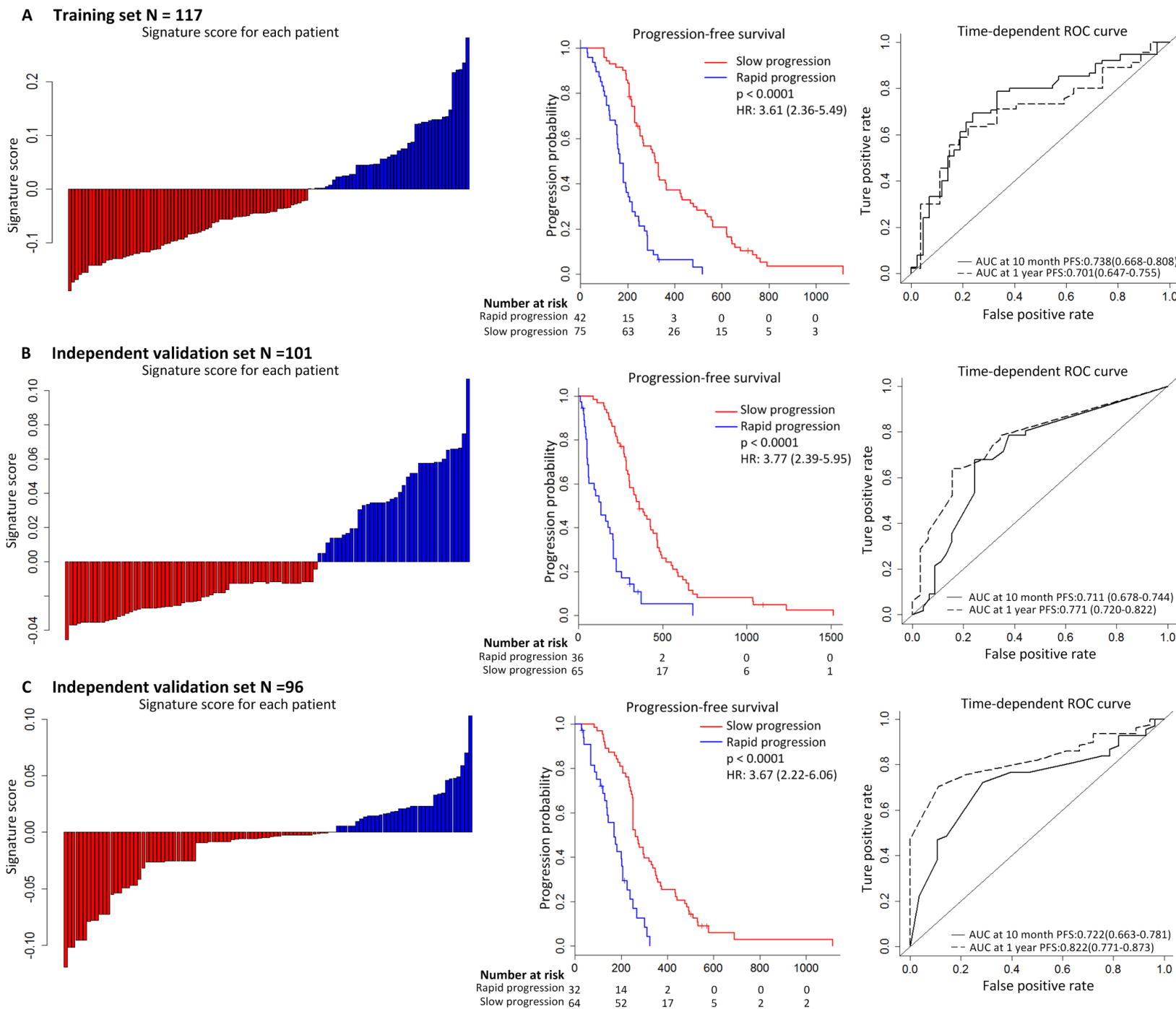


Figure 3

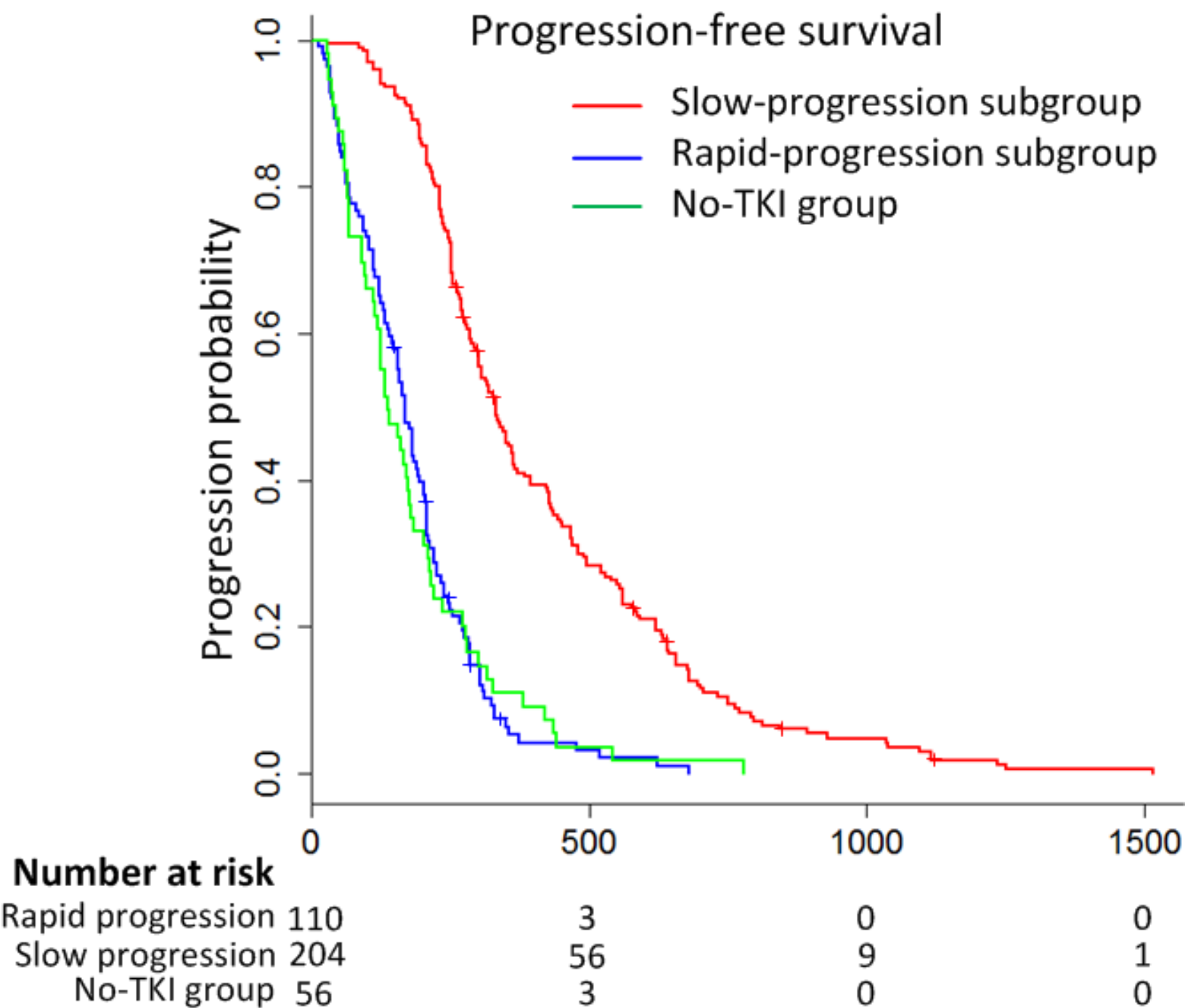
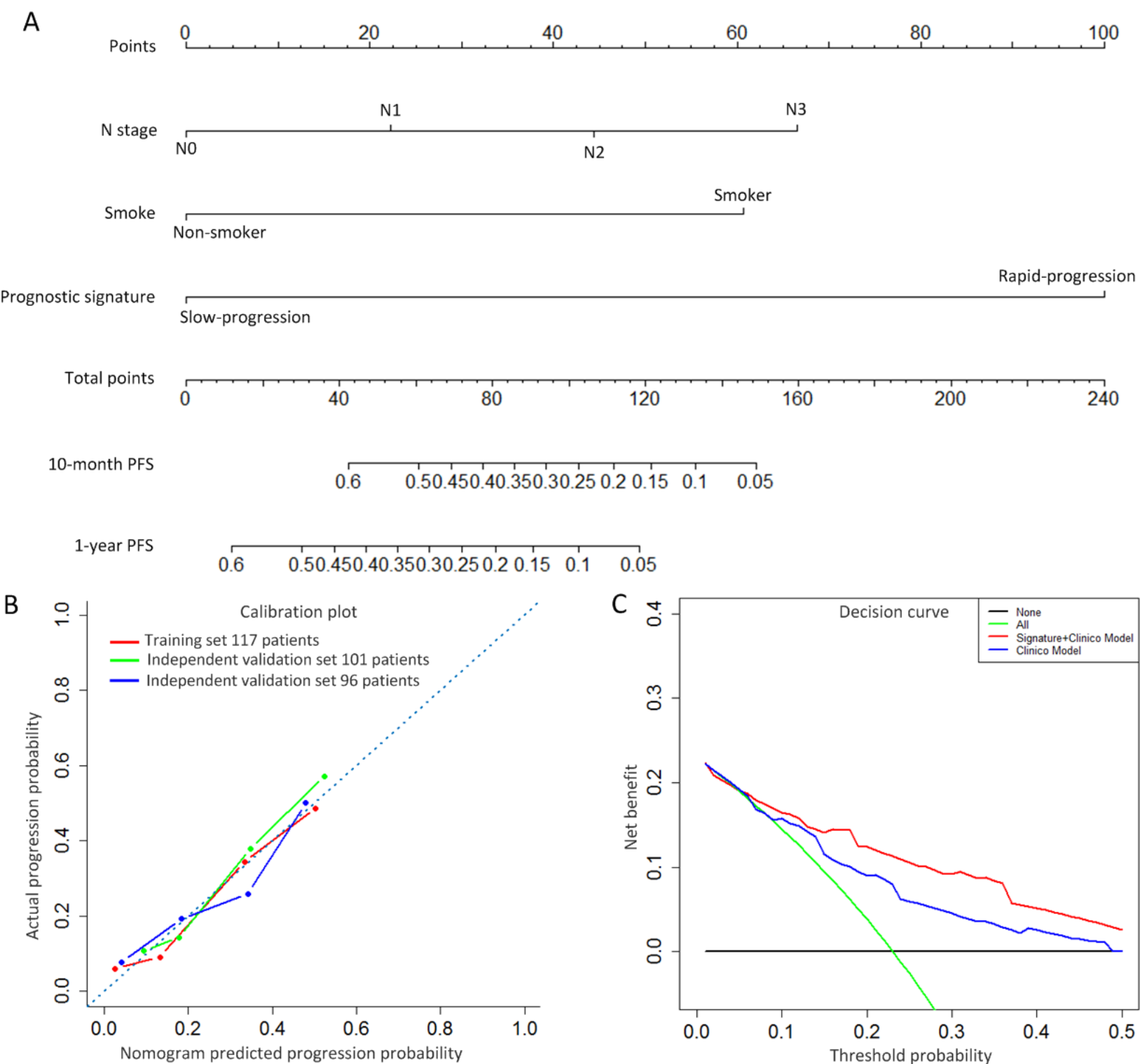


Figure 4



Clinical Cancer Research

A new approach to predict progression-free survival in stage IV EGFR-mutant NSCLC patients with EGFR-TKI therapy

Jiangdian Song, Jingyun Shi, Di Dong, et al.

Clin Cancer Res Published OnlineFirst March 21, 2018.

Updated version	Access the most recent version of this article at: doi: 10.1158/1078-0432.CCR-17-2507
Supplementary Material	Access the most recent supplemental material at: http://clincancerres.aacrjournals.org/content/suppl/2018/03/21/1078-0432.CCR-17-2507.DC1
Author Manuscript	Author manuscripts have been peer reviewed and accepted for publication but have not yet been edited.

E-mail alerts	Sign up to receive free email-alerts related to this article or journal.
Reprints and Subscriptions	To order reprints of this article or to subscribe to the journal, contact the AACR Publications Department at pubs@aacr.org .
Permissions	To request permission to re-use all or part of this article, use this link http://clincancerres.aacrjournals.org/content/early/2018/03/21/1078-0432.CCR-17-2507 . Click on "Request Permissions" which will take you to the Copyright Clearance Center's (CCC) Rightslink site.